Am J Cancer Res 2018;8(12):2564-2574
www.ajcr.us /ISSN:2156-6976/ajcr0087696

*Original Article*

# miR-338-3p targets *RAB23* and suppresses tumorigenicity of prostate cancer cells

Yuxiong Wang[1], Haiyan Qin[2]

[1]*Department of Urology, Shanghai Xuhui Central Hospital, Shanghai 200031, China;* [2]*Department of Radiation Oncology, First Affiliated Hospital, Guangzhou Medical University, Guangzhou 510120, Guangdong, China*

Received October 31, 2018; Accepted November 13, 2018; Epub December 1, 2018; Published December 15, 2018

**Abstract:** MicroRNA-338-3p (miR-338-3p) has been implicated in several cancers; however, its role in human prostate cancer remains unknown. In this study, we observed downregulation of miR-338-3p in prostate cancer tissues and cell lines. Forced expression of miR-338-3p suppressed prostate cancer cell proliferation, migration, and invasion *in vitro* and tumor growth *in vivo*, while apoptosis was induced. Further experiments revealed that *RAB23* is a target of miR-338-3p because miR-338-3p bound directly to the 3'-untranslated region (3'-UTR) of *RAB23* mRNA, thereby reducing both the mRNA and protein levels of RAB23. Reintroduction of RAB23 attenuated the inhibitory effects of miR-338-3p on proliferation, migration, and invasiveness of prostate cancer cells. In clinical samples, miR-338-3p levels negatively correlated with RAB23 expression, which was upregulated in prostate cancer. Collectively, these results indicate that miR-338-3p acts as a tumor suppressor in prostate cancer by directly targeting *RAB23*.

**Keywords:** miR-338-3p, prostate cancer, RAB23, tumorigenicity

## Introduction

Prostate cancer is a commonly diagnosed malignant tumor in the United States and is the second leading cause of cancer-related deaths among men worldwide [1]. Moreover, the incidence and lethality of prostate cancer steadily increase in many countries. Only in the United States, there were approximately 160,000 new diagnoses and 29,000 deaths due to prostate cancer in 2018 [1]. Great advances have been made in primary therapy of prostate cancer. Nonetheless, nearly all such patients develop castration-resistant prostate cancer after primary androgen deprivation therapy, which is the main treatment of prostate cancer [2]. Meanwhile, various mutations have been found to be associated with prostate cancer progression [3]. Therefore, it is urgently necessary to investigate the mechanism behind prostate cancer progression because this accomplishment will help to devise effective strategies for the diagnosis, treatment, and prognosis of prostate cancer.

MicroRNAs (miRNAs) are small noncoding RNAs, which perform a crucial function in various biological processes by regulating the translation of their target mRNAs [4, 5]. Several studies have shown that miRNAs can modulate the expression of a variety of genes involved in cancer progression. Increasing evidence also indicates that miRNAs could serve as either oncogenes or tumor suppressors in biological processes including cell proliferation, invasion, the cell cycle, and apoptosis, and therefore can contribute to tumorigenesis [6]. Some miRNAs have been found to be abnormally expressed during the initiation and progression of prostate cancer, for example, miR-193b, miR-466, miR-149-3p, and miR-1246 [7-10]. MiR-338-3p, which is encoded in chromosomal region 17q25, has been reported to be downregulated in certain cancers, including gastric cancer, non-small cell lung cancer, thyroid cancer, breast cancer, and hepatocellular carcinoma [11-15]. Nonetheless, the biological functions and molecular mechanisms underlying the effects of miR-338-3p on prostate cancer have yet to be elucidated.

In this study, we found that miR-338-3p expression is lower in prostate cancer tissues and cell lines. Overexpression of miR-338-3p inhibited

prostate cancer cell proliferation, migration, and invasion *in vitro* and tumorigenicity *in vivo*. As for the mechanism, the biological functions of miR-338-3p were found to be mediated by targeting of *RAB23* mRNA, whose expression turned out to be significantly increased in prostate cancer. Moreover, reintroduction of RAB23 attenuated the inhibitory effects of miR-338-3p on the proliferation, migration, and invasiveness of prostate cancer cells. These results provide a clearer understanding of the underlying mechanism by which miR-338-3p inhibits prostate cancer.

## Materials and methods

### *Patients and clinical tissue samples*

A total of 24 fresh prostate cancer tissue samples and matched normal prostate tissue samples were obtained at Shanghai Xuhui Central Hospital. All the samples were quickly frozen in liquid nitrogen for subsequent experiments. Written informed consent was obtained from all the patients. The protocol was approved by the Institutional Research Ethics Committee of Shanghai Xuhui Central Hospital.

### *Cell lines and cell culture*

Human prostate cancer cell lines PC-3, DU145, LNCap, 22RV1, and VCap, and normal prostate epithelial cell line RWPE-1 were purchased from the Cell Bank of Type Culture Collection (Shanghai, China). All the cell lines were cultured in the RPMI 1640 medium (Gibco BRL, Rockville, MD, USA) with 10% fetal bovine serum (Sigma, St. Louis, MO, USA), 100 U/ml penicillin, and 100 μg/ml streptomycin (Invitrogen, Carlsbad, CA, USA). All the cell lines were maintained in a 37°C humidified incubator in an atmosphere containing 5% $CO_2$.

### *Quantitative reverse transcription PCR (qRT-PCR)*

Total miRNA from cultured cells and tissues was extracted using the mirVana miRNA Isolation Kit (Ambion, Austin, TX, USA) and was reverse-transcribed by means of the Universal cDNA Synthesis Kit (Exiqon, Copenhagen, Denmark). qPCR was carried out with the SYBR® Green Master Mix (Exiqon). The expression levels of U6 and *GAPDH* served for normalization of the data. Relative expression levels of miR-338-3p and *RAB23* mRNA were determined by the $2^{-\Delta\Delta CT}$ method. All qRT-PCRs were performed at least three times on Light Cycler 480 System II (Roche Diagnostics, USA). The PCR primers for miR-338-3p were 5'-TCCAGCATCAGTGATT-3' and 5'-GTGCAGGGTCCGAGGT-3'. The PCR primers for U6 were 5'-GCGCGTCGTGAAGCGTTC-3' and 5'-GTGCAGGGTCCGAGGT-3'. The PCR primers for *RAB23* were 5'-GTGCTCGTGTTCTCTACC-3' and 5'-TGAATGCGTTAGTTCTGGAT-3'. The PCR primers for *GAPDH* were 5'-GGAGCGAGATCCCTCCAAAAT-3' and 5'-GGCTGTTGTCATACTTCTCATGG-3'.

### *Vector construction and lentivirus transduction*

The coding sequences of *RAB23* were cloned into pcDNA3.1(+) to generate a RAB23 expression vector. To construct a luciferase reporter vector, a fragment of wild-type (Wt) or mutant (Mt) 3'-UTR of *RAB23* was cloned into the firefly luciferase-expressing vector pmirGLO. A lentivirus expressing miR-338-3p was purchased from GenePharma (Shanghai, China). PC-3 and DU145 cells were transduced with the recombinant lentivirus in the presence of 10 μg/ml polybrene.

### *Cell proliferation and colony formation assays*

The 3-(4,5-dimethylthiazol-2-yl)-2,5-diphenyl tetrazolium bromide (MTT) assay was performed to assess cell proliferation. Briefly, cells were seeded in 96-well plates at $5 \times 10^3$/well. Then, 100 μl of a sterile MTT dye (0.5 mg/ml, Sigma) was added into each well and kept there for 4 h in a 37°C incubator. Three parallel wells were set up for each group of cells. After the supernatants were discarded, 150 μl of dimethyl sulfoxide was added into each well. The absorbance of each well was measured at 490 nm on a microplate reader. For colony formation assays, 500 cells were seeded in 6-well plates. After 10 days, the cells were fixed with 70% ethanol, stained with 10% Giemsa (Sigma-Aldrich), and counted under an inverted microscope. All the experiments were carried out in triplicate.

### *Migration and invasion assays*

The Transwell system was used to detect cell migration according to the manufacturer's protocols. For each well, $5 \times 10^4$ cells were seeded in the upper chamber of Transwell plates in a

serum-free RPMI 1640 medium, while the medium with 10% FBS was added into the lower compartment. The cells remaining in the upper chamber were scraped off, followed by fixation in methanol and staining with a 0.1% crystal violet solution after 48 h incubation. Five random visual fields were selected to count the cells that migrated to the lower side. For invasion assays, $10^5$ cells were seeded in the upper chambers coated with Matrigel®. The assay was then performed as the migration assay.

*Cell apoptosis assay*

A total of $3 \times 10^5$ cells were seeded in 6-well plates in triplicate, followed by incubation with an anti-annexin V antibody. After incubation for 15 min, 1.5 μl of propidium iodide (PI, 1 mg/ml, Sigma-Aldrich) was added into each well and incubated for 5 min. After that, the cells were analyzed using a FACSCalibur flow cytometer (BD Biosciences, San Jose, CA, USA).

*Luciferase reporter assay*

Cells were cotransfected with miRNA mimics and luciferase reporter plasmids. After 48 h, the cells were washed with PBS and lysed. Next, 20 μl of each lysate was analyzed via the Dual-Luciferase Reporter Assay System (Promega, Madison, WI) in a GloMax 96 Microplate luminometer. Three independent experiments were conducted.

*Western blotting and immunohistochemical (IHC) staining*

Proteins were isolated from cells by lysis in RIPA buffer and were quantified by means of the BCA Protein Assay Kit (Pierce, Rockford, IL, USA). The proteins in lysates were separated by SDS-PAGE in a 10% gel and were electrophoretically transferred to an Immobilon-P transfer membrane (Millipore). Then, the membranes were blocked with 5% nonfat milk and incubated with an anti-RAB23 antibody (1:500 dilution; Proteintech, 11101-1-AP, Wuhan, China) (primary antibody) overnight at 4°C. The membranes were incubated with a horseradish peroxidase-conjugated secondary antibody at room temperature for 1 h. The protein bands were detected with the ECL Plus Developing System. β-actin served as a control. To perform IHC staining, all the 5-μm-thick tissue sections fixed with formalin and embedded in paraffin were deparaffinized and rehydrated. After that, the sections were subjected to antigen retrieval with citrate buffer, followed by incubation with 0.3% $H_2O_2$ for 15 min, and were blocked with 5% BSA for 60 min. Next, the tissue sections were incubated with an antibody against RAB23 (1:100 dilution; Proteintech, 11101-1-AP) at 4°C overnight, followed by incubation with a secondary antibody at room temperature for 60 min. The immune complex was visualized by means of the DAB chromogen. The nuclei were counterstained with hematoxylin.

*Tumor xenograft model*

A total of $10^6$ PC-3 cells stably overexpressing miR-338-3p or control RNA were injected subcutaneously into flanks of 5-week-old male BALB/C nude mice (n = 6 per group). The tumor volumes were measured on days 7, 14, 21, and 28 after the implantation procedure. Tumor volume was calculated using the equation V ($mm^3$) = length × width$^2$/2. The tumors were collected for IHC staining. All animal studies were reviewed and approved by the Institutional Animal Care and Use Committee of Shanghai Jiaotong University.

*Statistical analysis*

Data were expressed as mean ± standard deviation (SD) from at least three separate experiments performed in triplicate. Statistical analyses were performed in SPSS 23.0 statistical software (SPSS Inc., Chicago, IL, USA). Differences between two groups were assessed by unpaired Student's *t* test, and the relation between miR-338-3p and RAB23 expression was evaluated by Pearson's correlation analysis. Data with $P < 0.05$ were considered significant.

## Results

*miR-338-3p is repressed in prostate cancer and serves as a prognostic factor in patients with prostate cancer*

We first analyzed miR-338-3p expression in human prostate cancer cell lines (PC-3, DU145, LNCaP, 22RV1 and VCaP) and in normal prostate epithelial cell line RWPE-1 to determine the involvement of miR-338-3p in prostate cancer. As shown in **Figure 1A**, miR-338-3p expression levels were significantly lower in prostate cancer cells than in RWPE-1 cells. We next com-

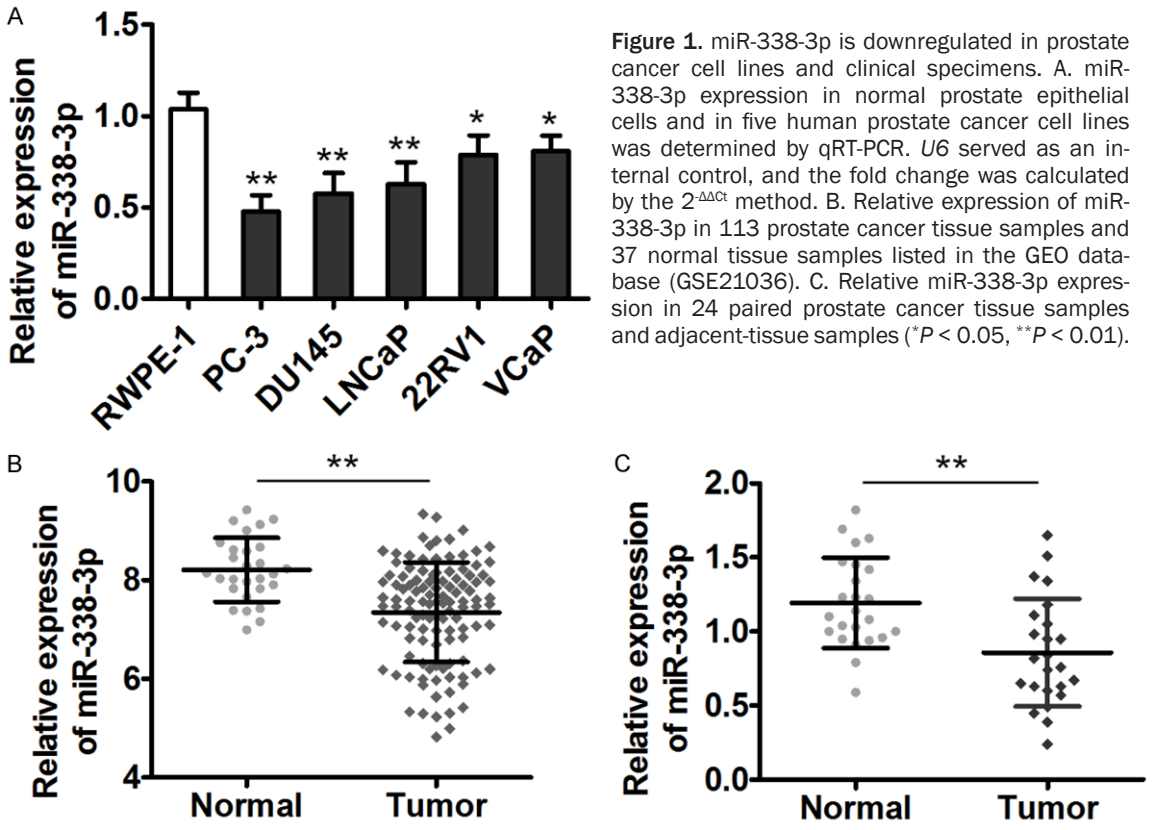


**Figure 1.** miR-338-3p is downregulated in prostate cancer cell lines and clinical specimens. A. miR-338-3p expression in normal prostate epithelial cells and in five human prostate cancer cell lines was determined by qRT-PCR. *U6* served as an internal control, and the fold change was calculated by the $2^{-\Delta\Delta Ct}$ method. B. Relative expression of miR-338-3p in 113 prostate cancer tissue samples and 37 normal tissue samples listed in the GEO database (GSE21036). C. Relative miR-338-3p expression in 24 paired prostate cancer tissue samples and adjacent-tissue samples ($^{*}P < 0.05$, $^{**}P < 0.01$).

pared miR-338-3p expression among 113 prostate cancer tissue samples and 37 normal prostate tissue samples using the GEO database. The expression level of miR-338-3p was significantly lower in prostate cancer tissues as compared with normal tissue samples (**Figure 1B**). We next analyzed miR-338-3p expression in 24 paired prostate cancer tissue samples and samples from healthy adjacent tissue. Consistent with the above observations, the average expression of miR-338-3p was obviously lower in prostate cancer tissues compared with adjacent tissues. These results suggested that miR-338-3p was downregulated in prostate cancer; it may function as a tumor suppressor in prostate cancer.

*miR-338-3p inhibits prostate cancer cell proliferation in vitro and xenograft tumor growth in vivo*

To further explore the functions of miR-338-3p in prostate cancer cells, we overexpressed miR-338-3p in PC-3 and DU145 cells using a lentivirus, and overexpression of miR-338-3p in these cells was confirmed by qRT-PCR (**Figure 2A**). MiR-338-3p overexpression strongly inhibited the viability of PC-3 and DU145 cells as compared to the controls (**Figure 2B**). Accordingly, miR-338-3p overexpression notably suppressed the colony formation ability of these cells because the colony number significantly decreased after miR-338-3p overexpression (**Figure 2C**). We next determined the effect of miR-338-3p on tumorigenicity *in vivo* by means of the xenograft model. PC-3 cells with overexpressed miR-338-3p or negative control (NC) RNA were injected into the flanks of nude mice. MiR-338-3p overexpression significantly suppressed prostate tumor growth, as evidenced by smaller tumor size 4 weeks after implantation (**Figure 2D**). In addition, we performed IHC staining for Ki67 in the tissue sections of xenograft tumors. The results showed that miR-338-3p overexpression decreased Ki67 expression (**Figure 2F** and **2G**). These results indicated that miR-338-3p could serve as a suppressor of prostate tumorigenesis.

*miR-338-3p promotes prostate cancer cell apoptosis and suppresses cell migration and invasion in vitro*

We next determined the influence of miR-338-3p on prostate cancer cell apoptosis. After miR-338-3p overexpression, apoptosis of PC-3 and

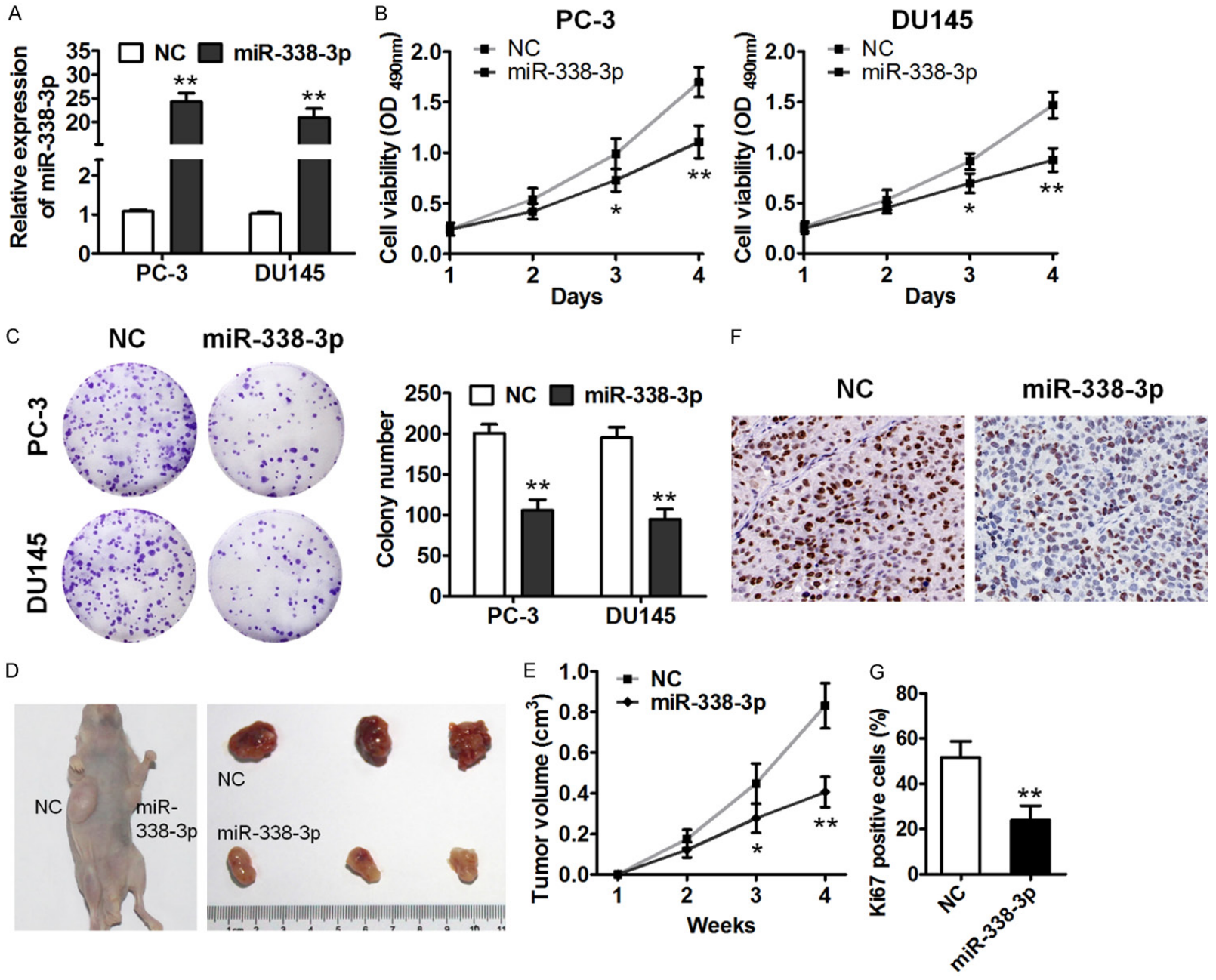
A
Relative expression of miR-338-3p
NC
miR-338-3p
PC-3
DU145
B
PC-3
DU145
Cell viability (OD 490nm)
Days
C
NC
miR-338-3p
PC-3
DU145
Colony number
D
NC
miR-338-3p
E
Tumor volume (cm3)
Weeks
F
G
Ki67 positive cells (%)

**Figure 2.** miR-338-3p inhibits prostate cancer cell proliferation *in vitro* and *in vivo*. A. qRT-PCR analysis of miR-338-3p expression in PC-3 and DU145 cells infected with the miR-338-3p-overexpressing lentivirus (indicated as "miR-338-3p") or a control lentivirus (indicated as "NC"). B. Cell viability was measured by the MTT assay of the indicated cells. C. The colony formation assay was performed on miR-338-3p-overexpressing PC-3 and DU145 cells. D. Subcutaneous tumors that were formed in nude mice by PC-3 cells stably overexpressing miR-338-3p or control RNA at 4 weeks after implantation (n = 6). E. Tumor volume of miR-338-3p-overexpressing cells at the indicated time points. F. IHC staining of Ki67 in the endpoint tumors. G. Percentages of Ki67-positive cells ($^{*}P < 0.05$, $^{**}P < 0.01$).

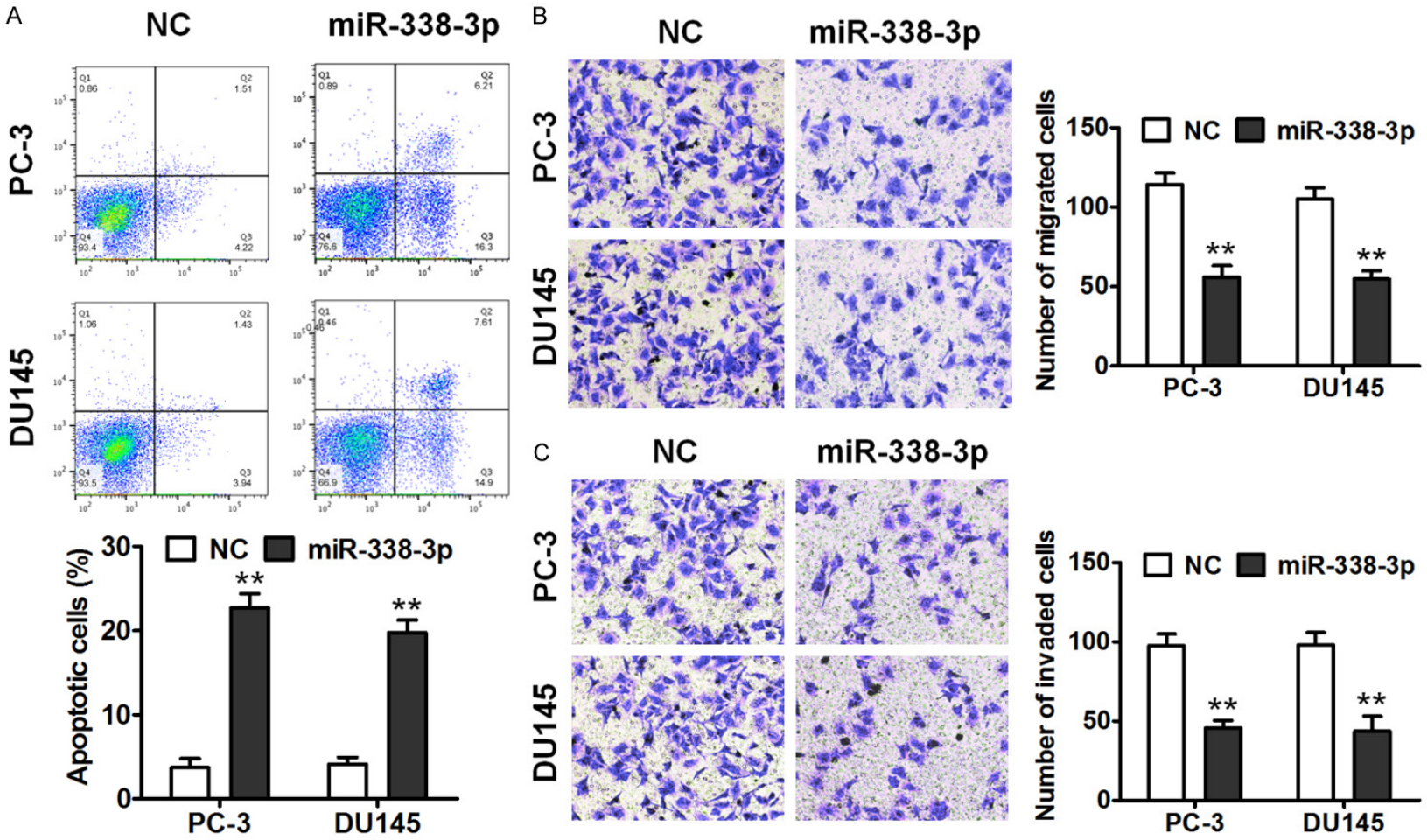


**Figure 3.** miR-338-3p promotes apoptosis and suppresses prostate cancer cell migration and invasion *in vitro*. A. The annexin V-FITC/PI apoptosis assay was performed to demonstrate the promotion of apoptosis by miR-338-3p in PC-3 and DU145 cells. B. The Transwell migration assay was conducted to measure the migration ability of the cells. C. The Transwell invasion assay was carried out to measure the cell invasion ability ($^{**}P < 0.01$).

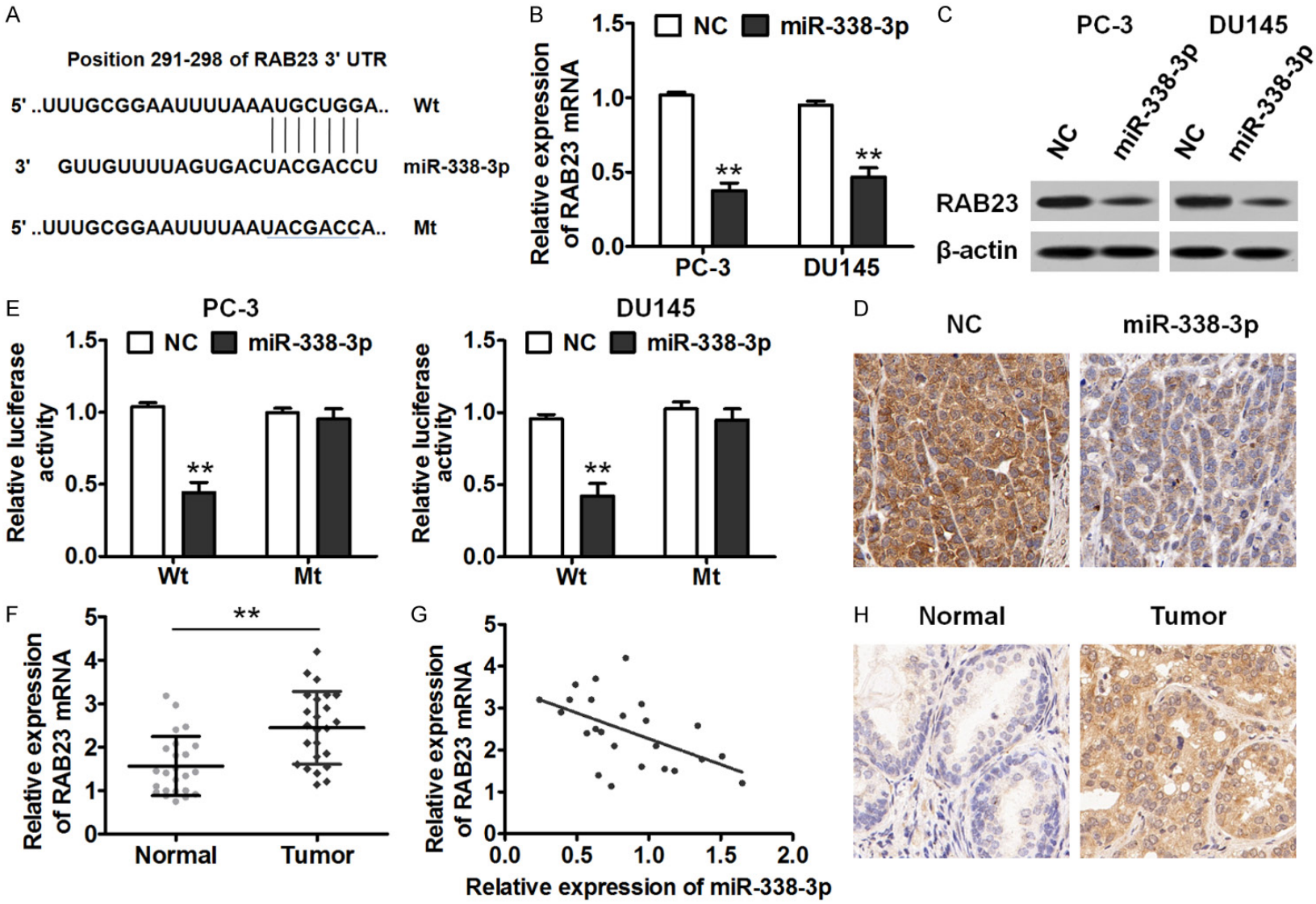


**Figure 4.** miR-338-3p suppresses RAB23 expression by directly targeting the 3'-UTR of *RAB23* mRNA. A. Sequence alignment of miR-338-3p and its predicted binding sites in *RAB23* 3'-UTR. B. Relative expression of *RAB23* mRNA was measured by qRT-PCR in PC-3 and DU145 cells infected with the miR-338-3p-overexpressing lentivirus or control lentivirus. C. Western blot analysis of *RAB23* expression in the indicated cells. D. IHC staining against RAB23 in the xenograft tumor tissues. E. A luciferase reporter assay. A vector containing Wt *RAB23* 3'-UTR or Mt *RAB23* 3'-UTR was cotransfected into prostate cancer cells together with the indicated oligonucleotides. A luciferase activity ratio is presented as firefly luciferase activity/*Renilla* luciferase activity. F. Relative expression of RAB23 mRNA in 24 paired

samples. G. Pearson's analysis of correlation between miR-338-3p and *RAB23* mRNA levels in human prostate cancer tissue samples (r = -0.532, $P = 0.007$). H. RAB23 protein expression in prostate cancer tissue samples was analyzed by IHC ($^{**}P < 0.01$).

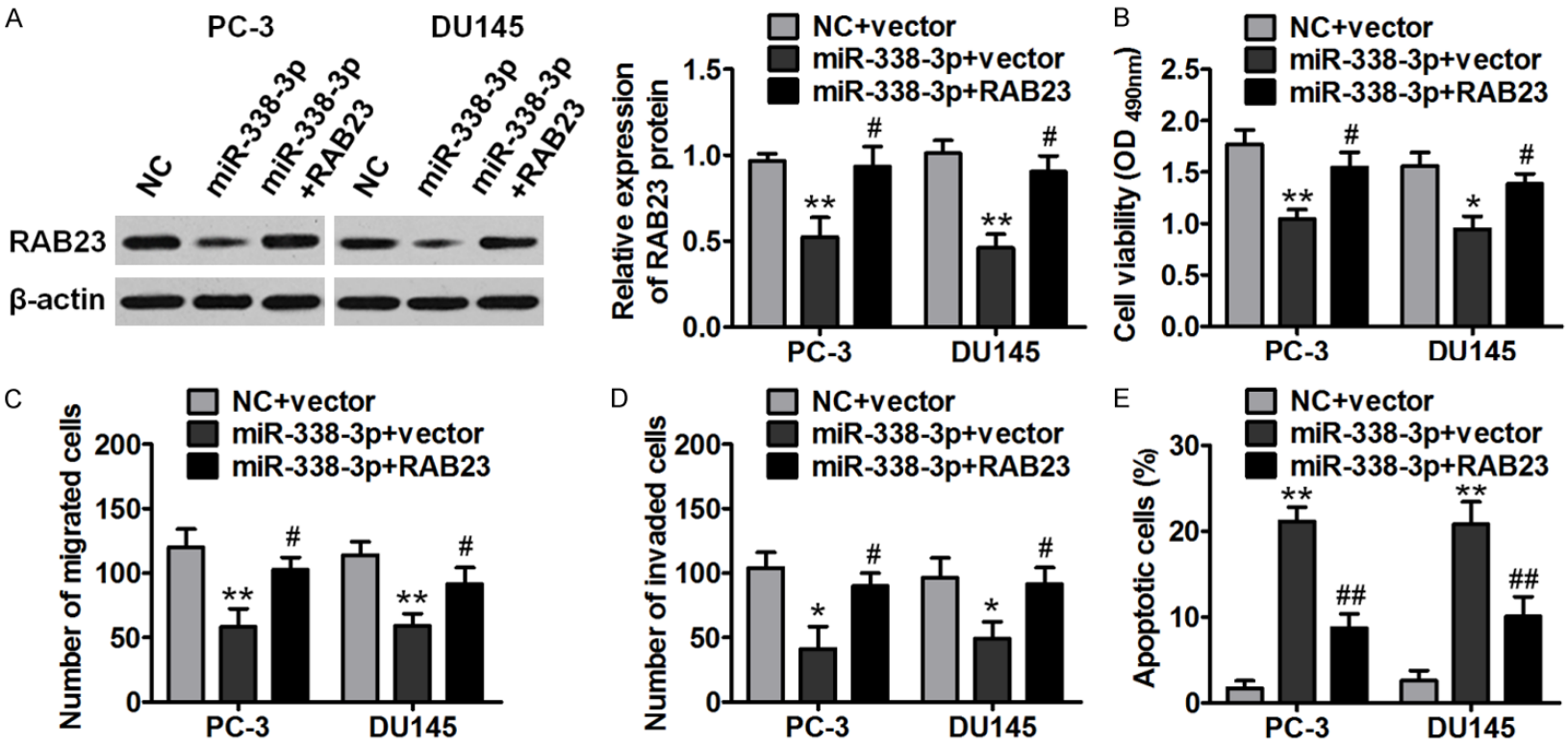


**Figure 5.** *RAB23* mediates the effects of miR-338-3p on the proliferation, migration, and invasiveness of prostate cancer cells. PC-3 and DU145 cells overexpressing miR-338-3p were transfected with a RAB23-overexpressing vector or control vector, and functional assays were then performed. A. Western blot analysis revealed that transfection of RAB23-overexpressing plasmids recovered the RAB23 expression in miR-338-3p-overexpressing PC-3 and DU145 cells. B-D. RAB23 overexpression reverted the suppressive effects of miR-338-3p overexpression on the proliferation, migration, and invasiveness of prostate cancer cells. E. RAB23 overexpression abrogated the effect of miR-338-3p on prostate cancer cell apoptosis ($^{*}P < 0.05$, $^{\#}P < 0.05$, $^{**}P < 0.01$).

DU145 cells significantly increased in comparison with NC cells as determined by annexin V-fluorescein isothiocyanate (FITC) and PI double staining (**Figure 3A**). In addition, the Transwell assay was performed to detect the effect of miR-338-3p on migration and invasiveness of PC-3 and DU145 cells. miR-338-3p overexpression significantly inhibited migration and invasiveness of PC-3 and DU145 cells (**Figure 3B** and **3C**). These results indicated that miR-338-3p promoted apoptosis and inhibited migration and invasiveness of the prostate cancer cell lines.

*RAB23 is a direct target of miR-338-3p in prostate cancer cells*

To investigate the molecular mechanism behind the biological roles of miR-338-3p in prostate cancer, we used TargetScan (a publicly available database) to predict the potential target of miR-338-3p, and *RAB23* was thus identified (**Figure 4A**). We next detected *RAB23* expression levels in PC-3 and DU145 cells with overexpressed miR-338-3p or NC RNA. After miR-338-3p overexpression, *RAB23* expression levels significantly decreased at both mRNA and protein levels (**Figure 4B** and **4C**). Similarly, IHC staining of the tumor tissues confirmed reduced RAB23 protein in miR-338-3p-overexpressed tumors compared to the control tumors (**Figure 4D**). To confirm that *RAB23* is the direct target gene of miR-338-3p, we next constructed luciferase reporter vectors containing Wt or Mt sequences of RAB23 3'-UTR. Luciferase activity in PC-3 and DU145 cells was much lower when these cells were transfected with the Wt sequence of *RAB23* 3'-UTR relative to the NC sequence. In contrast, when the cells were transfected with Mt sequences of *RAB23* 3'-UTR, there was no significant difference in luciferase activity between miR-338-3p and NC (**Figure 4E**), suggesting that *RAB23* is a direct target gene of miR-338-3p in prostate cancer cells. We next examined *RAB23* mRNA expression levels in prostate cancer tissues by qRT-PCR. As presented in **Figure 4F**, *RAB23* mRNA levels were much higher in prostate cancer tissue samples than adjacent normal tissue samples. In addition, there was a negative correlation between miR-338-3p and *RAB23* expression levels in prostate cancer tissue samples (**Figure 4G**). An IHC assay also indicated that *RAB23* expression levels were much higher in prostate cancer tissues than in normal tissue samples (**Figure 4H**). These data suggested that *RAB23* is a direct target gene of miR-338-3p in prostate cancer cells.

*miR-338-3p exerts its antitumor activity by suppressing RAB23 expression*

To further verify whether miR-338-3p exerts its activities by inhibiting RAB23 expression, we rescued RAB23 expression in miR-338-3p-overexpressing PC-3 and DU145 cells by transfecting these cells with RAB23 plasmids (lacking 3'-UTR). As depicted in **Figure 5A**, RAB23 rescue experiments successfully promoted RAB23 expression in cotransfected cells (miR-338-3p+RAB23). Moreover, RAB23 overexpression reversed the inhibitory effects of miR-381 overexpression on the proliferation, migration, and invasiveness of prostate cancer cells (**Figure 5B-D**). Furthermore, the apoptosis caused by miR-338-3p overexpression was attenuated by RAB23 overexpression (**Figure 5E**). These data meant that miR-338-3p performs its antitumor function by suppressing RAB23 expression.

## Discussion

Prostate cancer is becoming a major threat to men's health worldwide [1]. Therefore, how to find a biomarker of prostate cancer and the mechanism of prostate cancer progression need to be elucidated for effective treatment of this cancer. Here, we identified a novel miRNA, miR-338-3p, that is underexpressed in prostate cancer tissues. miR-338-3p overexpression was found here to suppress tumorigenicity of prostate cancer cells via targeting of *RAB23* mRNA. To the best of our knowledge, this is the first report of a crucial role of miR-338-3p in prostate cancer.

Aberrant miR-338-3p expression closely correlates with carcinogenesis [16]. miR-338-3p is frequently downregulated and acts as a tumor suppressor in several distinct cancer types. It has been demonstrated that miR-338-3p can inhibit cancer cell proliferation, migration, and invasion and induce cancer cell apoptosis by targeting multiple genes, including *PTP1B, IRS2, AKT3, EYA2* and *PKLR* [11-15], which are often amplified in human cancers and function as important regulators of cell growth and tumor invasion. Consistent with these findings,

our results revealed that miR-338-3p is downregulated in prostate cancer tissues and cell lines. Overexpression of miR-338-3p inhibited prostate cancer cell proliferation, migration, and invasion *in vitro* and tumorigenicity *in vivo*. Furthermore, via a publicly available database, *RAB23* was predicted here as a potential target gene of miR-338-3p.

RAB23 is a novel member of the Rab GTPase family and is associated with various types of tumors [17]. Overexpression of RAB23 has been uncovered in patients with hepatocellular carcinoma and gastric cancer and is known to be associated with tumor size [18]. Overexpression of RAB23 promotes hepatocellular carcinoma cell migration through the Rac1-TGF-β signaling pathway [19]. Another report has identified *RAB23* as a gene upregulated in human bladder cancer and promoting cancer cell proliferation and invasion [20]. As for prostate cancer, Chang and colleagues recently reported that RAB23 is overexpressed in tumor tissues and cell lines, and its downregulation remarkably suppresses tumor cell proliferation, migration, and invasion [21]. Consistent with these results, our findings in this study confirm that RAB23 expression is higher in clinical prostate cancer tissue samples and negatively correlates with miR-338-3p expression. miR-338-3p seems to directly target the 3'-UTR of *RAB23* mRNA and to suppress its expression at both mRNA and protein levels. Moreover, reintroduction of RAB23 attenuated the inhibitory effects of miR-338-3p on the characteristics of prostate cancer cells. These results establish a functional connection between miR-338-3p and RAB23 and confirm that miR-338-3p plays a tumor-suppressive part in prostate cancer cells by targeting RAB23. Nonetheless, RAB23 has also been reported to exert tumor-suppressive actions through inhibition of Gli1 and Gli2 expression in breast cancer [22]. The real reason for the two distinct effects of RAB23 is not clear yet; in part, it might be the organ-specific actions and the different cellular contexts of tumors.

In summary, we for the first time determined the participation of miR-338-3p in prostate cancer. MiR-338-3p overexpression inhibited the proliferation, migration, and invasiveness of prostate cancer cells *in vitro*, and attenuated tumorigenicity *in vivo*. In terms of the mechanism, the biological functions of miR-338-3p appear to be implemented via targeting of RAB23 mRNA. Altogether, miR-338-3p could function as a tumor suppressor in prostate cancer. The identification of miR-338-3p and its target gene RAB23 in prostate cancer would help in better understanding of the molecular mechanisms underlying prostate cancer development.

## Disclosure of conflict of interest

None.

**Address correspondence to:** Haiyan Qin, Department of Radiation Oncology, First Affiliated Hospital, Guangzhou Medical University, 151 Yanjiang Road, Guangzhou 510120, Guangdong, China. E-mail: wrhiou@126.com

## References

[1] Siegel RL, Miller KD and Jemal A. Cancer statistics, 2018. CA Cancer J Clin 2018; 68: 7-30.

[2] Wang C, Chen J, Zhang Q, Li W, Zhang S, Xu Y, Wang F, Zhang B, Zhang Y and Gao WQ. Elimination of CD4(low)HLA-G(+) T cells overcomes castration-resistance in prostate cancer therapy. Cell Res 2018; 28: 1103-1117.

[3] Shen MM and Abate-Shen C. Molecular genetics of prostate cancer: new prospects for old challenges. Genes Dev 2010; 24: 1967-2000.

[4] Garzon R, Calin GA and Croce CM. MicroRNAs in cancer. Annu Rev Med 2009; 60: 167-179.

[5] Liu J. Control of protein synthesis and mRNA degradation by microRNAs. Curr Opin Cell Biol 2008; 20: 214-221.

[6] Calin GA and Croce CM. MicroRNA signatures in human cancers. Nat Rev Cancer 2006; 6: 857-866.

[7] Torres-Ferreira J, Ramalho-Carvalho J, Gomez A, Menezes FD, Freitas R, Oliveira J, Antunes L, Bento MJ, Esteller M, Henrique R and Jeronimo C. MiR-193b promoter methylation accurately detects prostate cancer in urine sediments and miR-34b/c or miR-129-2 promoter methylation define subsets of clinically aggressive tumors. Mol Cancer 2017; 16: 26.

[8] Colden M, Dar AA, Saini S, Dahiya PV, Shahryari V, Yamamura S, Tanaka Y, Stein G, Dahiya R and Majid S. MicroRNA-466 inhibits tumor growth and bone metastasis in prostate cancer by direct regulation of osteogenic transcription factor RUNX2. Cell Death Dis 2017; 8: e2572.

[9] Bellazzo A, Di Minin G, Valentino E, Sicari D, Torre D, Marchionni L, Serpi F, Stadler MB, Taverna D, Zuccolotto G, Montagner IM, Rosato A, Tonon F, Zennaro C, Agostinis C, Bulla R,

Mano M, Del Sal G and Collavin L. Cell-autonomous and cell non-autonomous down-regulation of tumor suppressor DAB2IP by microRNA-149-3p promotes aggressiveness of cancer cells. Cell Death Differ 2018; 25: 1224-1238.

[10] Bhagirath D, Yang TL, Bucay N, Sekhon K, Majid S, Shahryari V, Dahiya R, Tanaka Y and Saini S. microRNA-1246 is an exosomal biomarker for aggressive prostate cancer. Cancer Res 2018; 78: 1833-1844.

[11] Sun F, Yu M, Yu J, Liu Z, Zhou X, Liu Y, Ge X, Gao H, Li M, Jiang X, Liu S, Chen X and Guan W. miR-338-3p functions as a tumor suppressor in gastric cancer by targeting PTP1B. Cell Death Dis 2018; 9: 522.

[12] Zhang P, Shao G, Lin X, Liu Y and Yang Z. MiR-338-3p inhibits the growth and invasion of non-small cell lung cancer cells by targeting IRS2. Am J Cancer Res 2017; 7: 53-63.

[13] Sui GQ, Fei D, Guo F, Zhen X, Luo Q, Yin S and Wang H. MicroRNA-338-3p inhibits thyroid cancer progression through targeting AKT3. Am J Cancer Res 2017; 7: 1177-1187.

[14] Liang Y, Xu X, Wang T, Li Y, You W, Fu J, Liu Y, Jin S, Ji Q, Zhao W, Song Q, Li L, Hong T, Huang J, Lyu Z and Ye Q. The EGFR/miR-338-3p/EYA2 axis controls breast tumor growth and lung metastasis. Cell Death Dis 2017; 8: e2928.

[15] Nie H, Li J, Yang XM, Cao QZ, Feng MX, Xue F, Wei L, Qin W, Gu J, Xia Q and Zhang ZG. Mineralocorticoid receptor suppresses cancer progression and the Warburg effect by modulating the miR-338-3p-PKLR axis in hepatocellular carcinoma. Hepatology 2015; 62: 1145-1159.

[16] Huang XH, Chen JS, Wang Q, Chen XL, Wen L, Chen LZ, Bi J, Zhang LJ, Su Q and Zeng WT. miR-338-3p suppresses invasion of liver cancer cell by targeting smoothened. J Pathol 2011; 225: 463-472.

[17] Chen Y, Ng F and Tang BL. Rab23 activities and human cancer-emerging connections and mechanisms. Tumour Biol 2016; 37: 12959-12967.

[18] Hou Q, Wu YH, Grabsch H, Zhu Y, Leong SH, Ganesan K, Cross D, Tan LK, Tao J, Gopalakrishnan V, Tang BL, Kon OL and Tan P. Integrative genomics identifies RAB23 as an invasion mediator gene in diffuse-type gastric cancer. Cancer Res 2008; 68: 4623-4630.

[19] Zhang L, Zhang B, You W, Li P and Kuang Y. Rab23 promotes hepatocellular carcinoma cell migration via rac1/TGF-beta signaling. Pathol Oncol Res 2018; [Epub ahead of print].

[20] Jiang Y, Han Y, Sun C, Han C, Han N, Zhi W and Qiao Q. Rab23 is overexpressed in human bladder cancer and promotes cancer cell proliferation and invasion. Tumour Biol 2016; 37: 8131-8138.

[21] Chang J, Xu W, Liu G, Du X and Li X. Downregulation of Rab23 in prostate cancer inhibits tumor growth in vitro and in vivo. Oncol Res 2017; 25: 241-248.

[22] Liu Y, Zeng C, Bao N, Zhao J, Hu Y, Li C and Chi S. Effect of Rab23 on the proliferation and apoptosis in breast cancer. Oncol Rep 2015; 34: 1835-1844.